



Gambogic Acid Mitigates Nephropathy by Inhibiting Oxidative Stress and Inflammation in Diabetic Rats

Ruttiya Thongrung¹ , Sarawut Lapmanee² , Penjai Thongnuanjan Bray³ ,
Patlada Suthamwong⁴ , Suwaporn Deandee¹ , Kanjana Pangjit^{1,5} , Chaowalit Yuajit^{1,5*}

1. College of Medicine and Public Health, Ubon Ratchathani University, Warin Chamrap, Ubon Ratchathani, 34190 Thailand.

2. Division of Physiology, Chulabhorn International College of Medicine, Thammasat University, Khlong Luang, Pathum Thani, 12120 Thailand.

3. Toxicology Graduate Program, Multidisciplinary Unit, Faculty of Science, Mahidol University, Bangkok, 10400 Thailand.

4. Department of Agronomy, Faculty of Agriculture, Ubon Ratchathani University, Warin Chamrap, Ubon Ratchathani, 34190 Thailand.

5. Research Group for Biomedical Research and Innovative Development (RG-BRID), College of Medicine and Public Health, Ubon Ratchathani University, Warin Chamrap, Ubon Ratchathani, 34190 Thailand.

Article type: ABSTRACT

Original Article

Diabetic nephropathy is a leading cause of end-stage renal disease globally, with limited treatment options to prevent its progression. Gambogic acid (GA), a xanthone isolated from *Garcinia hanburyi*, has shown notable anti-oxidative, anti-inflammatory, and anti-proliferative properties. This study aimed to assess GA's renoprotective effects in a model of diabetic nephropathy mediated by low dose streptozotocin (STZ) combined with a high-fat diet, focusing on its potential to reduce oxidative stress and inflammation. Control-treated vehicle and STZ/high-fat diet-mediated diabetic rats were administered either the vehicle or 3 or 6 mg/kg of GA to assess its effects on renal inflammation, fibrosis, and oxidative stress. Renal histological changes were assessed, and markers for inflammation and oxidative stress, including I- κ B α , p-p38/MAPK, and p-p65NF- κ B pathways, were measured to explore the mechanisms of GA. Diabetic rats showed significant renal dysfunction, structural damage, and increased inflammation and fibrosis. Treatment with GA markedly improved renal structure and function. GA also reduced oxidative stress, increased I- κ B α expression, and inhibited key signaling pathways, specifically p-p38/MAPK and p-p65NF- κ B, involved in cellular inflammation. GA exhibits promising renoprotective effects in diabetic nephropathy by reducing oxidative stress and inflammation, supporting its potential as a natural therapeutic agent for diabetic renal disease.

Received:
2024.11.18

Revised:
2024.12.11

Accepted:
2024.12.21

Keywords: Gambogic acid, Cell inflammation, Diabetic rat, p38/MAPK, NF- κ B

Cite this article: Thongrung R, *et al.* Gambogic Acid Mitigates Nephropathy by Inhibiting Oxidative Stress and Inflammation in Diabetic Rats. *International Journal of Molecular and Cellular Medicine*. 2025; 14(1):448-461.

DOI: 10.22088/IJMCM.BUMS.14.1.448

*Corresponding: Chaowalit Yuajit

Address: College of Medicine and Public Health, Ubon Ratchathani University, Warin Chamrap, Ubon Ratchathani, 34190 Thailand.

E-mail: chaowalit.y@ubu.ac.th



© The Author(s).

Publisher: Babol University of Medical Sciences

This work is published as an open access article distributed under the terms of the Creative Commons Attribution 4.0 License (<http://creativecommons.org/licenses/by-nc/4>). Non-commercial uses of the work are permitted, provided the original work is properly cited.

Introduction

Diabetic kidney disease (DKD), a microvascular complication, commonly occurs in type 2 diabetes mellitus and hypertension patients after 10–15 years (1). Hyperglycemia directly stimulates high glomerular filtration and increases the number of extracellular mesangial cells, which further activates oxidative stress and inflammatory processes in nephrons (2). These changes can result in the thickening of the glomerular barrier and renal tubules, leading to the development of glomerulosclerosis and tubulointerstitial fibrosis. Ultimately, this may cause a decrease in renal function, leading to end-stage renal diseases. Pathophysiology of diabetic nephropathy (DN) involves increased oxidative stress, cellular inflammation, and fibrosis, which affect several signaling pathways (3). Previous report suggests that proinflammatory cytokines, such as interleukin 1 β and TNF- α , stimulate renal inflammation through the p-p38/MAPK and p-p65NF- κ B pathways (4). In addition, increased levels of reactive oxygen species induce the p-ERK1/2 and TGF β /Smad pathways, which further stimulate renal interstitial fibrosis (5). Therefore, inhibiting inflammatory processes in DN may retard the progression of renal disease to chronic kidney disease (CKD).

To develop nutraceuticals for the treatment of CKD, it is crucial to elucidate the detailed mechanisms of novel plant-based candidates, based on the underlying pathophysiology of CKD. Gambogic acid, GA, is a xanthone derivative isolated from the yellowish-brown resin of *Garcinia hanburyi* tree (6). GA has demonstrated several biological activities, including anti-proliferative (7), anti-cancer (8), anti-metastasis (9), anti-angiogenesis (10), anti-inflammatory (11), and apoptosis-inductive activities (12). In non-small cell lung carcinoma, GA inhibits cell inflammation and necrosis by reducing p-NF- κ B expression (13). Additionally, GA was found to inhibit angiogenesis in renal cell carcinoma (14). Interestingly, GA significantly suppresses angiogenesis by inhibiting the PI3K/AKT signaling in a diabetic retinopathy mice model (15). GA also suppresses renal fibrosis by inhibiting Smad7-mediated TGF β /Smad3 signaling in mouse renal epithelial cells (16). Furthermore, a cell model of DN revealed that GA protects against high glucose-induced renal epithelial cell damage by suppressing pyroptosis via regulation of the AMPK-TXNIP signaling (17). We hypothesized that the renoprotective effects of GA on oxidative stress and inflammation could retard the progression of diabetic renal injury. Therefore, this study was to investigate the potential of GA in preventing the deterioration of renal function by targeting pathways associated with oxidative stress and inflammation in an *in vivo* model of type 2 diabetic renal injury.

Materials and methods

Chemical reagents

GA was obtained from Calbiochem (San Diego, USA). Streptozotocin was also obtained from Calbiochem (San Diego, USA). The protease inhibitor cocktail was purchased from Hoffman-La Roche Ltd. (Basel, Switzerland). Enhanced chemiluminescence solution was obtained from Calbiochem (San Diego, USA) for protein detection. The cytokine (TNF- α) enzyme-linked immunosorbent assay kit was obtained from Abcam (Cambridge, UK) to detect TNF- α protein levels. Primary antibodies, including anti-p-p38 (Thr180/Tyr182), anti-p38, anti-p-p65NF- κ B (Ser536), anti-p65NF- κ B, anti-I κ B α , anti- β -actin, and anti-rabbit IgG horseradish peroxidase-linked antibody, were obtained from Cell Signaling (Beverly, USA).

Animal and treatments

Animal experiments were conducted at the Animal Center of Thammasat University, Thailand. The Institutional Animal Care and Use Committee of Thammasat University approved the animal study protocol (approval number: 021/2021). Male Wistar rats, weighing 200–300 g with aged 8–10 weeks, were performed in this study. According to the diabetic protocol from Lapmanee *et al.* (18), a single intraperitoneal (i.p.) injection of streptozotocin (35 mg/kg body weight (BW)) was administered to partially destroy pancreatic β -cells and induce diabetes. The STZ-induced diabetic rats were maintained on a high-fat diet (HFD32), comprising 32% crude fat and 60% of total calories derived from fat, sourced from CLEA Japan, Inc. (Tokyo, Japan). The diet was provided starting after the acclimatization period. After 1-week STZ injection, fasting blood glucose levels were measured to diagnose diabetes, defined as a level greater than 180 mg/dL. Diabetic rats were then fed a high-fat diet *ad libitum*, which was maintained throughout the duration of the study. The study consisted of four experimental groups, each with 8 rats: normal control, vehicle- treated DN, and GA-treated DN groups which was divided into two subgroups (i.e., 3 and 6 mg/kg) (Figure 1). GA was dissolved in 0.1% DMSO, and diabetic rats were administered GA at concentrations of 3 and 6 mg/kg via i.p. injection daily for 4 weeks. For the 24-hour urine collection, animals were housed in metabolic cages. Urine samples were then centrifuged at 2,000 rpm for 15 minutes at room temperature, and the supernatant was stored at -80°C until used for assaying kidney function parameters (i.e., albumin). At the end of the experiment, all rats fast

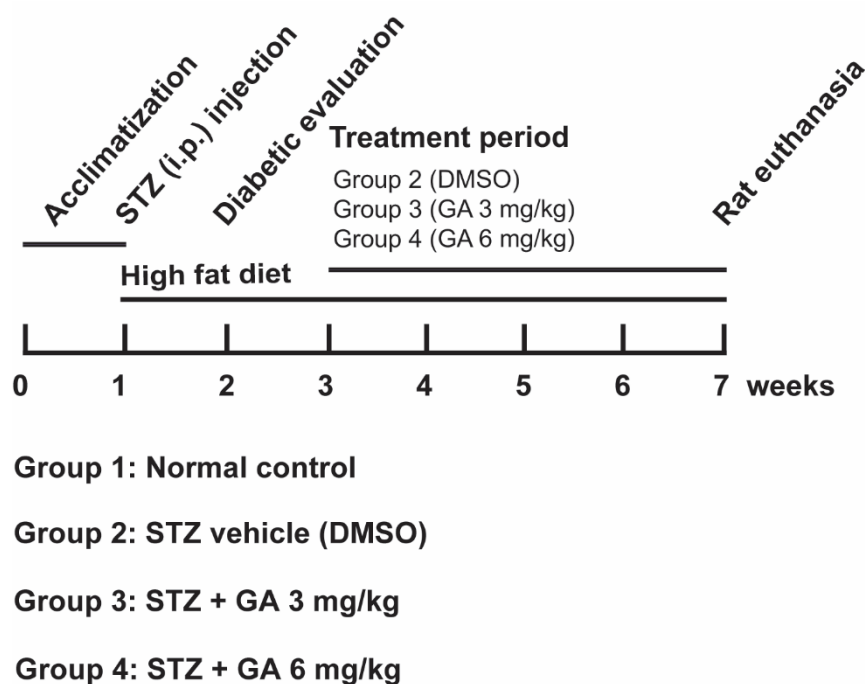


Fig. 1. Experimental procedures in streptozotocin/ high-fat diet-mediated type 2 diabetic rats. Following an acclimatization period, diabetes was induced in rats with a single intraperitoneal (i.p.) injection of streptozotocin (STZ; 35 mg/kg) combined with a high-fat diet. Seven days after STZ administration, plasma glucose levels were measured, and rats with glucose levels exceeding 180 mg/dL were confirmed as diabetic. Subsequently, the diabetic rats continued on the high-fat diet in parallel with GA treatment. Rat was randomly divided into 4 groups including normal control group ($n = 8$), diabetic vehicle group ($n = 8$), diabetic rat treated with GA at dose of 3 mg/kg BW ($n = 8$), and diabetic rat treated with GA at dose of 6 mg/kg for 4 weeks, respectively.

overnight to measure fasting blood glucose levels. Blood glucose concentrations were determined using an electronic glucometer. Glycated hemoglobin (HbA1c) levels were calculated as a direct indicator of blood glucose levels using the HbA1c calculator, based on the guidelines of the national glycohemoglobin standardization program.

After the animals were humanely euthanized using an i.p. injection of sodium pentobarbital, blood was collected, and the organs, including the kidneys, were carefully removed. Blood was collected, prepared, and centrifuged to measure creatinine and blood urea nitrogen (BUN) levels using an automatic biochemistry analyzer. Serum insulin levels were measured using an ELISA kit (Merck Millipore, Darmstadt, Germany) according to the manufacturer's protocol. All the kidneys were removed and weighed by a digital weight scale. Specifically, the right kidney was isolated, cleaned, and fixed in 4% paraformaldehyde. Following fixation, the kidney was embedded in paraffin and then cut into sagittal sections for histological staining and analysis, while the left kidney was stored and kept in an -80°C freezer until antioxidant and cytokine assays and Western blot analysis.

Histological analysis

Kidneys were embedded in paraffin. Sections were stained with hematoxylin and eosin (H&E), periodic acid-Schiff (PAS), and Masson's trichrome. Glomerular volume was determined by measuring thirty randomly selected glomeruli in each tissue slice, with calculations based on a specific formula. The extent of PAS staining was assessed by selecting ten random glomeruli from each tissue slice, followed by the calculation of percentage of PAS-positive substance within area of the glomeruli. Collagen deposition was evaluated using Masson's trichrome staining (MTS), with examination conducted in ten high-power fields. Furthermore, interstitial lesion, encompassing inflammatory infiltration, was scored based on the percentages of lesion frequency relative to the total number of images examined.

Antioxidation assays

Kidney tissues were collected from all experiments and rinsed with ice-cold 0.9% normal saline solution (NSS). Subsequently, kidney was homogenized using 100 mM PBS at a ratio of 5 mL/g of the kidney and then centrifuged at 12,000 g at 4 °C. The supernatant was further examined for oxidative stress biomarkers. Kidney lipid peroxidation was assayed by thiobarbituric acid reactive substance (TBARS). The kidney homogenate was mixed with 10% trichloroacetic acid (TCA), 8% sodium dodecyl sulfate (SDS), 5 mM ethylenediaminetetraacetic acid (EDTA) containing butylated hydroxytoluene (BHT). 0.6% TBA was added and heated for 30 min, and then was centrifuged at 10000 g at room temperature for 5 min. The supernatant was measured by a spectrophotometer at 532 nm. Kidney malondialdehyde (MDA) was determined using a standard curve of 1,1,3,3 tetra-ethoxypropane (0.3-1 µmol/L), and an MDA concentration was normalized against the protein concentration, which was evaluated using the Bradford dye binding method. While, the enzymatic activity of catalase (CAT) was determined via the CAT activity assay measures CAT levels. The reaction, in which catalase decomposes hydrogen peroxide (H₂O₂), was quickly stopped by the addition of ammonium molybdate. The residual H₂O₂ reacts with ammonium molybdate to generate a yellowish complex. CAT activity was calculated based on the production of this yellowish complex, with absorbance measured at 405 nm after incubation at 37 °C for 1 minute. Enzymatic activity was determined using a CAT standard curve.

Cytokine assay

The kidneys were extracted in a lysis buffer (NP-40/Triton X-100 lysis buffer), which contained 50 mM Tris-HCl (pH 8.5), 120 mM NaCl, 5 mM EDTA, 1% detergent (NP-40/Triton X-100), and protease inhibitors. The samples were centrifuged at 10,000×g. The level of cytokine production, specifically that of TNF- α , was measured in the supernatant collected from the kidney samples. This measurement was conducted using an ELISA kit according to the manufacturer's instructions.

Western blot analysis

Kidneys were homogenized and extracted using an ice-cold buffer containing 1 mM EDTA, 25 mM imidazole, 0.3 M sucrose and a protease inhibitor. The samples were centrifuged at 10,000×g, the supernatant (60 μ g) was separated by 10% SDS-PAGE. Proteins were transferred onto a nitrocellulose membrane and blocked with 5% non-fat dry milk. The membrane was incubated with primary antibodies (IkB α , p-p38, p38, p-p65NF- κ B, p65NF- κ B, β -actin) overnight at 4 °C, and subsequently, it was incubated with rabbit secondary antibodies. Finally, the immunoreactive band was developed using an ECL solution, and the resulting data were presented as a percentage of the band intensity of the interested protein between the GA treatment and control groups.

Statistical analysis

All data are presented as the mean \pm SEM. Statistical significance between the control and treatment groups was examined using a one-way analysis of variance, followed by Bonferroni's post hoc test. A *p*-value of less than 0.05 was considered statistically significant.

Results

GA slowed renal disease progression in STZ/high-fat diet-mediated diabetic rats.

To investigate the potential renoprotective effects of GA in type 2 diabetic rats, the experiment involved daily injections of GA at 3 and 6 mg/kg BW or vehicle into diabetic rats for 4 weeks. The parameters for

Table 1. GA ameliorates nephropathy progression in streptozotocin/high-fat diet-mediated type 2 diabetic rats.

Characteristic	NC (<i>n</i> = 8)	DMV (<i>n</i> = 8)	DMV + GA (3 mg/kg) (<i>n</i> = 8)	DMV + GA (6 mg/kg) (<i>n</i> = 8)
Body weight (g)	416.12 \pm 10.13	448.50 \pm 9.98	386.25 \pm 13.18	359.62 \pm 9.15**
Kidney weight (g)	1.36 \pm 0.04	1.4 \pm 0.05	1.33 \pm 0.02	1.23 \pm 0.04
K/W ratio	0.32 \pm 0.01	0.31 \pm 0.01	0.34 \pm 0.01	0.34 \pm 0.01
FBS (mL/dL)	157.75 \pm 2.93	194.00 \pm 5.27***	158.57 \pm 3.90###	163.87 \pm 3.52###
HbA1C (%)	6.60 \pm 0.08	7.62 \pm 0.14***	6.62 \pm 0.10###	6.77 \pm 0.98###
Serum insulin (μ g/mL)	6.56 \pm 0.82	2.58 \pm 0.55***	4.16 \pm 0.39 [#]	5.87 \pm 0.32###
SCr (mg/dL)	0.45 \pm 0.10	0.94 \pm 0.01***	0.81 \pm 0.02 [#]	0.69 \pm 0.02###
BUN (mg/dL)	17.58 \pm 0.81	24.68 \pm 2.13***	20.74 \pm 0.96	23.14 \pm 0.68
Urine albumin (mg/24 h)	3.29 \pm 0.28	25.20 \pm 0.40***	16.18 \pm 1.06 [#]	15.38 \pm 2.52##

Notes: Data were expressed as mean \pm SEM, *n* = 8, ***P* < 0.01, ****P* < 0.001 compared to that of normal control, [#]*P* < 0.05, ###*P* < 0.01, ####*P* < 0.001 compared to that of DM vehicle. **Abbreviations:** NC, normal control; DMV, diabetic vehicle; GA, gambogic acid; K/W, kidney weight per body weight ratio; FBS, fasting blood sugar; HbA1C, glycosylated hemoglobin; SCr, serum creatinine; BUN, blood urea nitrogen.

determining renal disease progression, including body weight, kidney weight, fasting FBS, serum BUN, serum creatinine, and 24 h urine albumin levels, were analyzed. The results showed that the higher body weight in the diabetic group compared to that of control could indicate diabetes-associated weight gain. GA treatment at 3 mg/kg BW may help mitigate this, while the 6 mg/kg BW significantly reverses the body weight gain (Table 1). In addition, GA at 3 and 6 mg/kg BW did not alter kidney weight or kidney weight ratio, indicating that it did not cause nephrotoxicity. FBS and HbA1C levels were elevated in diabetic rats, suggesting mild hyperglycemia. However, GA treatment reduced FBS and HbA1C levels, decreased urine albumin, and increased insulin levels compared to those in vehicle-treated diabetic rats (Table 1). The study also found that GA treatment improved renal function, as determined by significantly decreased serum creatinine, but not BUN levels, compared with those of vehicle diabetic group. These results suggest that GA slows renal disease progression and markedly improves kidney function by reducing FBS and creatinine levels in STZ/high-fat diet-mediated type 2 diabetic rats.

GA reduced renal histological alterations in STZ/high-fat diet-mediated diabetic rats.

The histological characteristics of renal in normal, diabetic, and diabetic-treated with GA rats were shown in Figure 2. The H&E results found that the histological of glomeruli appeared to enlarge in STZ-mediated diabetic rats compared to those of normal rats (Figure 2A). In diabetic rats treated with GA (3 and 6 mg/kg BW), did not present with glomerular abnormalities, but showed decreased glomerular volume (Figure 2B). Moreover, PAS staining represented the mesangial matrix of kidney reduced in STZ/high-fat diet-mediated type 2 diabetic rats and GA (3 mg/kg BW) treated diabetic rat restored the mesangial matrix of kidney (Figure 2A-C). Interestingly, GA (3 mg/kg BW) was found to suppress the deposition of connective tissue and collagen in the kidneys demonstrated by MTS, compared to those in diabetic rats treated with the vehicle (Figure 2A-D). In addition, GA (3 mg/kg BW) suppressed inflammatory cell infiltrate, which indicated interstitial lesion (Figure 2E). These findings suggest that GA improved morphological alterations such as glomerulopathy and interstitial lesions which slows diabetic renal injury.

GA showed anti-oxidative and anti-inflammatory effects on renal epithelial cells in STZ/high-fat diet-mediated diabetic rats.

To demonstrate the anti-oxidative effects of GA, lipid peroxidation and catalase activity assays were evaluated. The results demonstrated that GA at 3 and 6 mg/kg mildly reduced the concentration of MDA in diabetic rats compared to that in vehicle diabetic rats (Figure 3A). Furthermore, GA significantly elevated the catalase enzyme activity at both doses (Figure 3B). These findings suggest that GA impedes diabetic renal injury via its anti-oxidative properties.

The anti-inflammatory effects of GA were determined using an ELISA kit. The results revealed that GA at 3 and 6 mg/kg BW significantly ameliorated TNF- α level compared to that of vehicle diabetic rats (Figure 3C). These results suggest that GA alleviates diabetic renal injury through its anti-inflammatory action.

GA inhibited renal inflammation by inhibiting p38/MAPK and NF- κ B signaling in STZ/high-fat diet-mediated diabetic rats.

Western blot analysis was used to investigate the precise mechanism by which GA suppresses cell inflammation. Since diabetes-induced inflammation, the activation of I κ B α results in the suppression of phosphorylation of and p65NF- κ B. This result indicates that GA administration at 3 and 6 mg/kg strongly

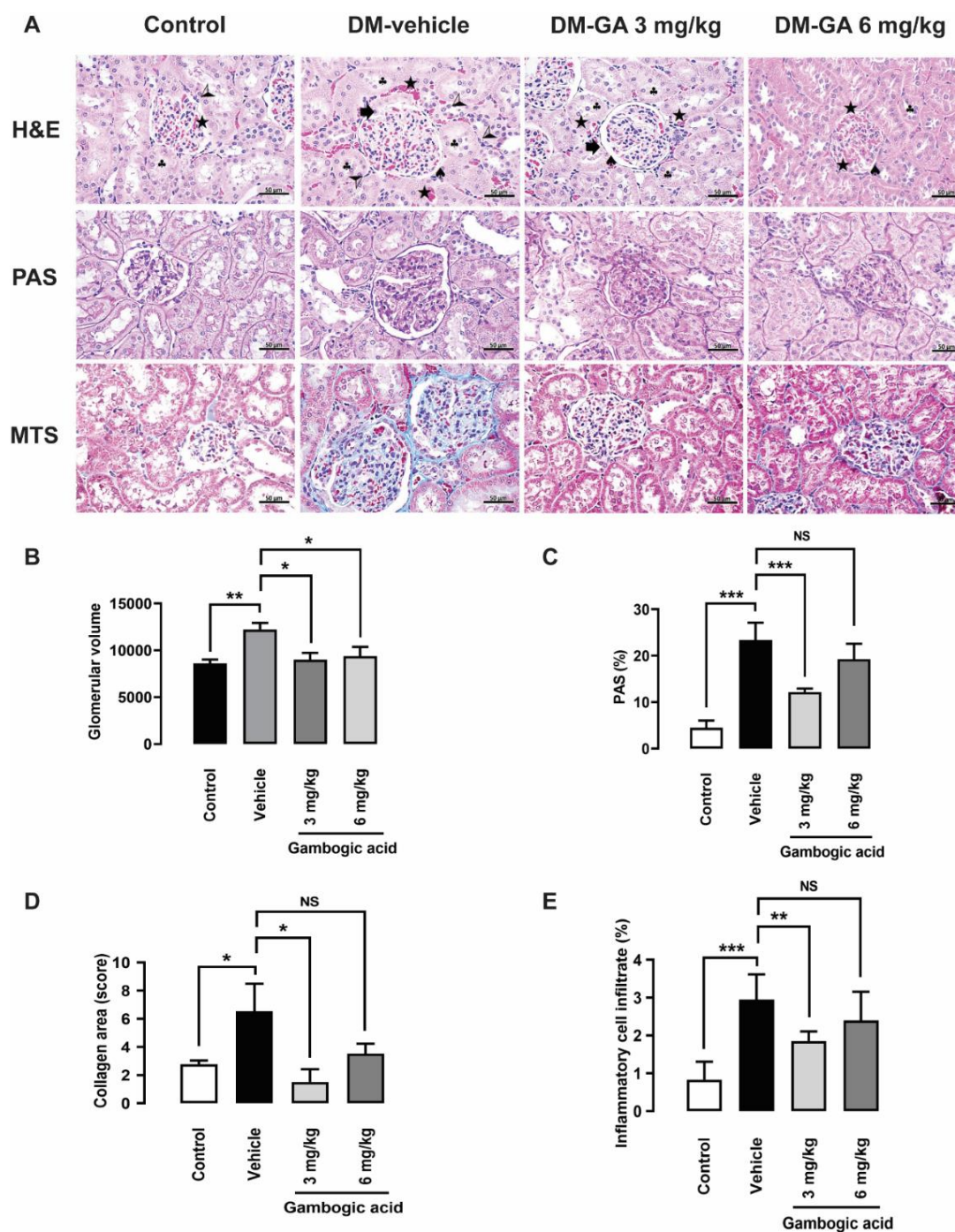


Fig. 2. Effect of GA on renal histological pathology in streptozotocin/high-fat diet-mediated type 2 diabetic rat. (A) Representative micro graphs of hematoxylin and eosin (H&E), periodic acid-Schiff (PAS), and Masson's trichrome staining (MTS). → represents congestion, ▲ represent shrinkage, ♣ represents swelling, ★ represent hemorrhage, ◀ represents interstitial inflammatory infiltrate. Original magnification 400×. (B) Graphs showing quantitative data of glomerular volume in normal rats (control), diabetic rats (vehicle), and GA at doses of 3 and 6 mg/kg BW (GA-treated). (C) Graphs showing quantitative data of PAS in normal rats (control), diabetic rats (vehicle), and GA at doses of 3 and 6 mg/kg BW (GA-treated). (D) Graphs showing quantitative data of collagen area in normal rats (control), diabetic rats (vehicle), and GA at doses of 3 and 6 mg/kg BW (GA-treated). (E) Graphs showing quantitative data of inflammatory cell filtration in normal rats (control), diabetic rats (vehicle), and GA at doses of 3 and 6 mg/kg BW (GA-treated) (mean % control ± SEM; $n = 4$, * $P < 0.05$, ** $P < 0.01$, *** $P < 0.001$; NS, not significant).

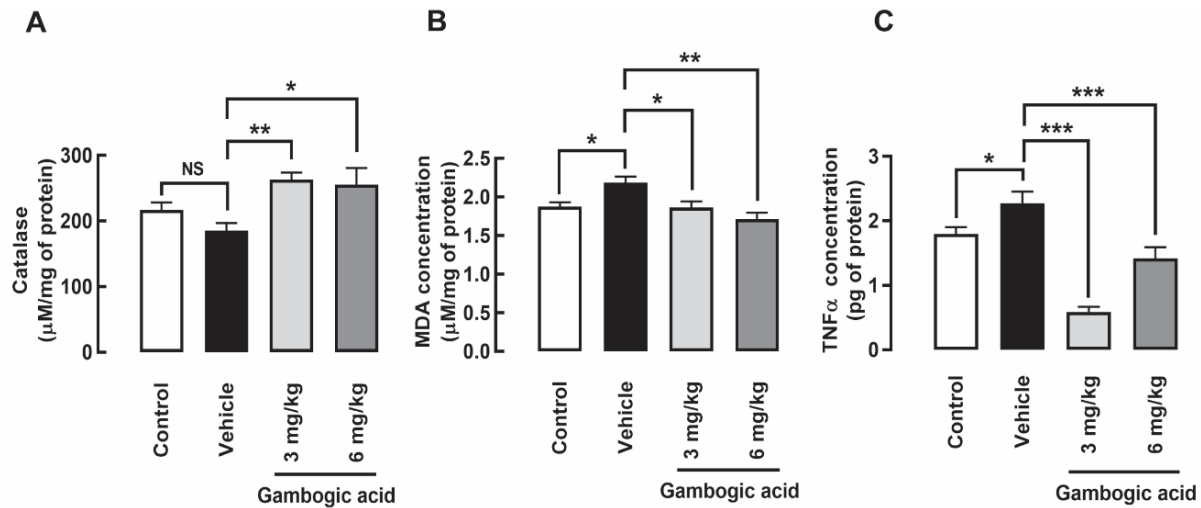
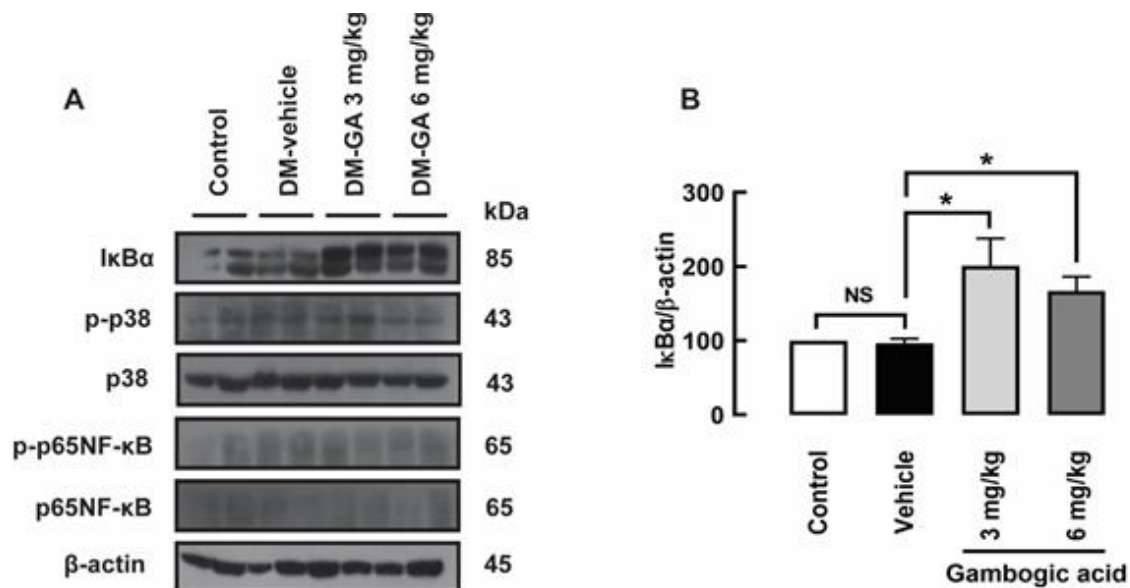


Fig. 3. Antioxidative effect and anti-inflammatory effect of GA in streptozotocin/high-fat diet-mediated type 2 diabetic rats. Lipid peroxidation and catalase enzyme activity were assessed. (A) Graphs showing quantitative data of catalase enzyme activity in normal rats (control), diabetic rats (vehicle), and GA at doses of 3 and 6 mg/kg BW (GA-treated). (B) Graphs showing quantitative data of MDA concentration in normal rats (control), diabetic rats (vehicle), and GA at doses of 3 and 6 mg/kg BW (GA-treated). (C) Graphs showing quantitative data of TNF- α concentration in normal rats (control), diabetic rats (vehicle), and GA at doses of 3 and 6 mg/kg BW (GA-treated) (mean % control \pm SEM; *n* = 4–5, **P* < 0.05, ***P* < 0.01, ****P* < 0.001; NS, not significant).

increased I κ B α expression (Figure 4 A-B). Moreover, GA diminished the expression of phosphorylation of both p38/MAPK and p65NF- κ B in renal epithelial cell of diabetic rats (Figure 4A, C-D). These findings collectively suggest that GA can retard diabetic renal progression, at least in part, by impeding cell inflammation through the attenuation of the p38/MAPK and p65NF- κ B signaling pathways.



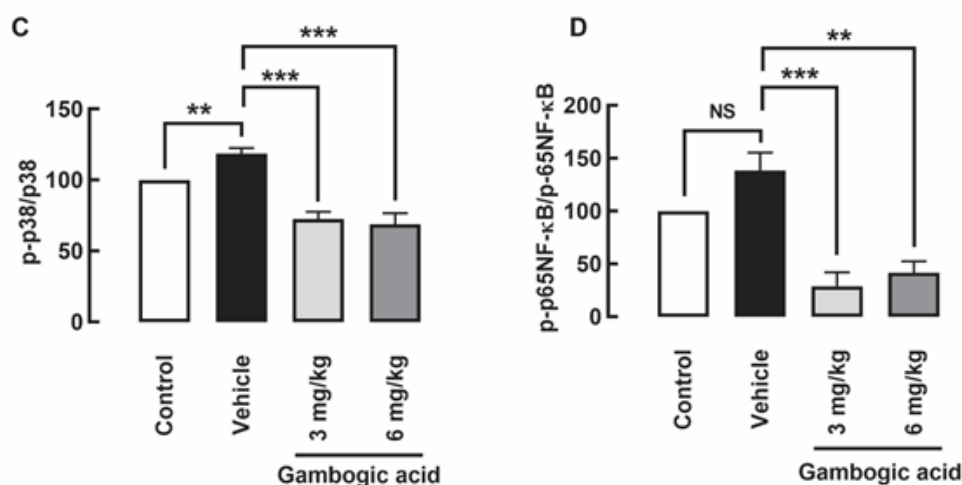


Fig. 4. Effect of GA on cell inflammation pathway in renal epithelial cell of streptozotocin/high-fat diet-mediated type 2 diabetic rats. (A) Proteins in kidney lysates were assessed by western blot analysis. Representative bands of I κ B α , p-p38, p38, p-p65NF- κ B, p65 NF- κ B, and β -actin are shown. Band intensity is represented as a histogram of indicated proteins including I κ B α / β -actin (B), p-p38/p38 (C), and p-p65NF- κ B/p-65 NF- κ B (D) in the normal rat (control), diabetic rat (vehicle), and GA at doses of 3 and 6 mg/kg BW (GA-treated). Data are expressed as mean of 100 %control \pm SEM; 6 independent experiments; $n = 6$, * $P < 0.05$, ** $P < 0.01$, *** $P < 0.001$; NS, not significant.

Discussion

This study uncovers a novel mechanism through which GA safeguards against renal injury in STZ-mediated diabetic rats. Presently findings illustrate that GA effectively preserved renal histological morphology and improved renal function in streptozotocin/high-fat diet-mediated type 2 diabetic model, showcasing its antioxidative effects and the significant reduction in cell inflammation by targeting the phosphorylation of p38/MAPK and p65NF- κ B signaling pathways.

STZ administration initiated β cell destruction and diminished insulin secretion in rats, followed by 4 weeks of a high-fat diet, leading to diabetes-like symptoms, including polyuria, polydipsia, and hyperglycemia (19). Despite only slight increases in plasma sugar levels in diabetic rats, substantial disparities emerged in renal structural and functional parameters when compared to normal rats. These differences encompassed elevated FBS, serum creatinine, BUN levels, albuminuria, as well as decreased serum insulin accompanied by renal inflammation, structural abnormalities, and fibrosis, thus establishing a valid model for DN. This model aligns with previous studies that employed streptozotocin with or without a high-fat diet to induce diabetes in animals, which are widely used for drug discovery research related to diabetes mellitus and diabetic nephropathy (18, 20-22).

GA was reported as an antitumor activity. It potently inhibited several types of tumors (8). Furthermore, GA and a structurally related compounds, i.e., gambogenic acid revealed a decrease in hepatotoxicity, plasma glucose levels, and a slower disease progression in cell and animal models of diabetes, both with and without retinopathy (15, 23, 24). However, the effect of GA to slow renal progression in DN has not reported. Our previous study revealed GA retarded renal cystogenesis by inhibiting Pkd1 mutant and MDCK cells proliferation pathway in cell model of polycystic kidney disease (25). It would be interesting to investigate

whether GA can retard the progression of DKD. This study determined the effect of GA on renal disease progression in STZ/high-fat diet-mediated diabetic rats. After 4 weeks of treatment, GA administered at 3 and 6 mg/kg BW could elevate serum insulin levels and reduced plasma glucose levels compared to vehicle diabetic rats. This is novel evidence proving that the GA have the potential in enhancing insulin levels and lowering plasma sugar levels in STZ damaged β cells in rats. In line with this notion, previous study was reported that GA decreased plasma glucose level in diabetic retinopathy which alleviated the severity of the disease. Additionally, renal function, as indicated by serum creatinine levels and albuminuria, improved with GA treatment compared to vehicle-treated diabetic rats. Histological analysis revealed that GA, at both doses, reduced histological injury, oxidative stress, and inflammation. These results are consistent with a previous study reporting that GA could decelerate the progression of diabetic retinopathy in RF/6A cells and mice (15).

The pathogenesis of DKD involves increased oxidative stress, cellular inflammation, and fibrosis, ultimately leading to renal structural damage, histological decline, and chronic kidney disease (5). DN exhibits characteristic histological changes such as glomerulosclerosis, interstitial fibrosis, tubular injury, and mononuclear cell infiltration. The histological examination of diabetic rats in this study revealed mesangial matrix accumulation in glomeruli, increased glomerular volume, and collagen fiber deposition, with concomitant mononuclear cell infiltration, consistent with previous studies (26, 27). The glomerular hyperfiltration is the feature of early stage of DN due to glomerular barrier damage or increased intraglomerular pressure leading to enlarge of glomerular volume (28). The beneficial effect of GA in reducing renal disease progression in diabetic rats is closely associated with glycemic regulation, suggesting that GA preserves renal structure and prevents histological changes by lowering plasma glucose levels as well as increasing insulin secretion, thereby reducing hyperfiltration in glomerular capillaries. Therefore, GA treatment effectively preserved renal structure, ameliorating these histological changes in diabetic rats.

Our investigation into the effects of GA on DN in rats demonstrated its capacity to reduce oxidative stress, suppress inflammation, and mitigate fibrosis, aligning with a previous study indicating that GA prevent angiotensin II-mediated abdominal aortic aneurysm by inhibiting oxidative stress and inflammation (29). In addition, Schisandrin B, a natural compound from *Schisandra chinensis*, attenuates DN by suppressing oxidative stress and inflammation via NF- κ B and Nrf2, leading to improved urinary clearance in diabetic mice (30). The NF- κ B plays an important role in inflammation by stimulating the transcription of factors, i.e., MCP1, TNF- α , and interleukins. Western blotting was performed to elucidate the mechanism underlying GA's effects on renal disease progression. We found that GA upregulated I κ B α protein expression which act as an inhibitor of NF- κ B and inhibited the phosphorylation of p38/MAPK and p65NF- κ B pathways. These findings correlate well with previous research showing that GA suppressed inflammation by inhibiting NF- κ B and MAPK pathway by activating Nrf2 signaling in LPS-induced Raw264.7 cells (31). Moreover, another anti-inflammatory drug, Thalidomide, effectively inhibits TGF- β /Smad, MCP1, and NF- κ B pathways, thereby suppressing inflammation and fibrosis in DN (32). Therefore, GA inhibited inflammation and oxidative stress by diminishing NF- κ B and p38/MAPK pathway might involve in Nrf2 signaling in diabetic rat which requires further study to examine this pathway.

As shown in our findings, GA administered at 6 mg/kg led to reduced body weight (Table 1), while no significant change was found in the kidney weight ratio. These findings suggest that the high dose of GA used in this study may contribute to general cytotoxic effects, potentially leading to reduced appetite, increased energy expenditure, or enhanced catabolic processes. However, previous studies have reported no cytotoxic effects of daily GA administration at 60 mg/kg over 13 weeks on kidney and liver tissues in rats (33). Additionally, a chronic toxicity in rats demonstrated that body weight decreased during weeks 3–4 when receiving 8 mg/kg of GA (34). Interestingly, in patients with advanced or metastatic cancer, a dose of 45 mg/m² GA administered intravenously 5 times a week for 2 weeks was well tolerated (35). Moreover, GA at doses of 1.5, 3, and 6 mg/kg was able to slow the progression of retinopathy without causing cytotoxicity in STZ-mediated diabetic mice (15). Therefore, a further study is required to elucidate the potential cytotoxic effects of high doses of GA in diabetic rat models.

The dose-dependent effect of GA on insulin levels likely arises from a multifaceted interplay of mechanisms and could also be influenced by individual variability. This intricate relationship between GA and insulin regulation is of significant interest, as it has implications for conditions characterized by aberrant insulin function. The impact of GA on insulin levels may involve stimulating beta cell activity and enhancing glucose uptake at lower doses, resulting in improved insulin sensitivity and increased insulin secretion, as investigated in ARPE-19 cells exposed to high glucose (24). Conversely, at higher doses, rats treated with GA had liver damage (33, 34), with liver toxicity correlating with pancreatitis (36). This could potentially have toxic effects on beta cells, disrupt glucose uptake mechanisms, lead to insulin resistance, or even excessively suppress the immune system, affecting insulin action (37). Furthermore, the role of GA in generating oxidative stress and modulating cellular signaling pathways, including those involved in insulin signaling (i.e., PI3K/Akt pathway), adds complexity to its dose-dependent effects.

Presumably, our diabetic model induced a mild diabetic condition, which had a lesser effect on the development of glomerulopathy, as typically observed in DN. A possible mechanism is that the single low dose of STZ that was used in this study partly destroyed a whole beta cell of the pancreas. In addition, GA might inhibit the effect of STZ in destroying beta cells in the islets, thereby stimulating insulin secretion.

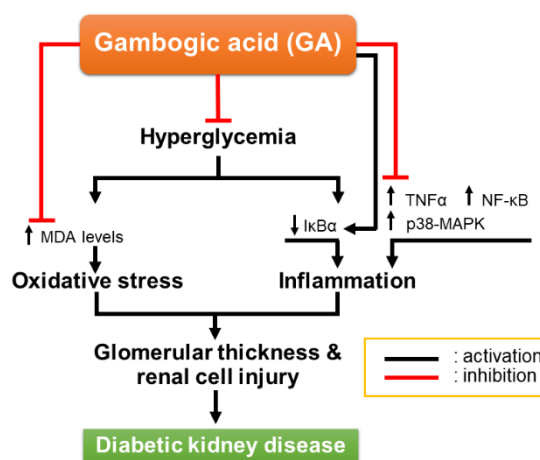


Fig 5. Possible mechanisms underlying the effects of GA on the inhibition of renal oxidative stress and inflammation in streptozotocin/high-fat diet-mediated type 2 diabetic rat.

In conclusions, the present study established the renoprotective effect of GA by reducing hyperglycemia, oxidative stress as well as inflammation, which represents a novel mechanism for slowing renal disease progression in STZ/high-fat diet-mediated type 2 diabetic rats. Specifically, GA has been shown to increase I κ B α and inhibit the p-p38/MAPK and p-p65NF- κ B signaling pathways (Figure 5). Nevertheless, additional studies are required to fully investigate the inhibitory mechanisms of GA in animal models of CKD such as cisplatin-induced nephrotoxicity and lipopolysaccharide-induced CKD. These findings suggest that GA could serve as a promising plant-based drug candidate for treating CKD caused by diabetes.

Acknowledgements

This work was supported by the administration and research service at Ubon Ratchathani University (grant to CY, FF2565). We would like to thank Miss Siriwan Sriwong and Mr. Napadol Suttirak from the Animal Laboratory Center at Thammasat University for their exceptional care in animal welfare and tissue preservation throughout this study.

References

1. Pérez-Morales RE, Del Pino MD, Valdivielso JM, et al. Inflammation in Diabetic Kidney Disease. *Nephron* 2019; 143: 12-6.
2. Navarro-González JF, Mora-Fernández C, Muros de Fuentes M, et al. Inflammatory molecules and pathways in the pathogenesis of diabetic nephropathy. *Nat Rev Nephrol* 2011; 7:327-40.
3. Xiong Y, Zhou L. The Signaling of Cellular Senescence in Diabetic Nephropathy. *Oxid Med Cell Longev* 2019; 2019:7495629.
4. Wang X, Li C, Huan Y, et al. Diphenyl diselenide ameliorates diabetic nephropathy in streptozotocin-induced diabetic rats via suppressing oxidative stress and inflammation. *Chem Biol Interact* 2021; 338:109427.
5. Kanasaki K, Taduri G, Koya D. Diabetic nephropathy: the role of inflammation in fibroblast activation and kidney fibrosis. *Front Endocrinol (Lausanne)* 2013; 4:7.
6. Liesenklas W, Auterhoff H. [The constitution of gambogic acid and its isomerization. 4. Chemistry of gum-resin]. *Arch Pharm Ber Dtsch Pharm Ges* 1966; 299:797-8.
7. Wang T, Du J, Kong D, et al. Gambogic acid inhibits proliferation and induces apoptosis of human acute T-cell leukemia cells by inducing autophagy and downregulating β -catenin signaling pathway: Mechanisms underlying the effect of Gambogic acid on T-ALL cells. *Oncol Rep* 2020; 44: 1747-57.
8. Liu Y, Chen Y, Lin L, et al. Gambogic Acid as a Candidate for Cancer Therapy: A Review. *Int J Nanomedicine* 2020; 15: 10385-99.
9. Li CY, Wang Q, Wang XM, et al. Gambogic acid exhibits anti-metastatic activity on malignant melanoma mainly through inhibition of PI3K/Akt and ERK signaling pathways. *Eur J Pharmacol* 2019; 864:172719.
10. Yi T, Yi Z, Cho SG, et al. Gambogic acid inhibits angiogenesis and prostate tumor growth by suppressing vascular endothelial growth factor receptor 2 signaling. *Can Res* 2008; 68:1843-50.
11. Wang QL, Yang DZ, Lv C. Anti-inflammatory effects of gambogic acid in murine collagen-induced arthritis through PI3K/Akt signaling pathway. *Mol Med Rep* 2018; 17:4791-6.
12. Yu Z, Jv Y, Cai L, et al. Gambogic acid attenuates liver fibrosis by inhibiting the PI3K/AKT and MAPK signaling pathways via inhibiting HSP90. *Toxicol Appl Pharmacol* 2019; 371:63-73.

13. Wang LH, Li Y, Yang SN, et al. Gambogic acid synergistically potentiates cisplatin-induced apoptosis in non-small-cell lung cancer through suppressing NF- κ B and MAPK/HO-1 signalling. *Br J Cancer* 2014; 110:341-52.
14. Jiang XL, Zhang Y, Luo CL, et al. Targeting renal cell carcinoma with gambogic acid in combination with sunitinib in vitro and in vivo. *Asian Pacific journal of cancer prevention: APJCP* 2012; 13:6463-8.
15. Cui J, Gong R, Hu S, et al. Gambogic acid ameliorates diabetes-induced proliferative retinopathy through inhibition of the HIF-1 α /VEGF expression via targeting PI3K/AKT p.athway. *Life sciences* 2018; 192:293-303.
16. Tao S, Yang L, Wu C, et al. Gambogenic acid alleviates kidney fibrosis via epigenetic inhibition of EZH2 to regulate Smad7-dependent mechanism. *Phytomedicine* 2022; 106:154390.
17. Li N, Wen X, Tang M, et al. Gambogenic acid protects against high glucose-induced damage of renal tubular epithelial cells by inhibiting pyroptosis through regulating the AMPK–TXNIP pathway. *Qual Assur Saf Crops Foods* 2022; 14:40-6.
18. Lapmanee S, Bhuhhanil S, Wongchitrat P, et al. Assessing the Safety and Therapeutic Efficacy of Cannabidiol Lipid Nanoparticles in Alleviating Metabolic and Memory Impairments and Hippocampal Histopathological Changes in Diabetic Parkinson's Rats. *Pharmaceutics* 2024; 16.
19. Ghasemi A, Jeddi S. Streptozotocin as a tool for induction of rat models of diabetes: a practical guide. *EXCLI journal* 2023; 22:274-94.
20. Zheng C, Huang L, Luo W, et al. Inhibition of STAT3 in tubular epithelial cells prevents kidney fibrosis and nephropathy in STZ-induced diabetic mice. *Cell death & disease* 2019; 10:848.
21. Li X, Wang Y, Wang K, et al. Renal protective effect of Paeoniflorin by inhibition of JAK2/STAT3 signaling pathway in diabetic mice. *Bioscience trends* 2018; 12:168-76.
22. Andonova M, Dzhelebov P, Trifonova K, et al. Metabolic Markers Associated with Progression of Type 2 Diabetes Induced by High-Fat Diet and Single Low Dose Streptozotocin in rats. *Vet Sci* 2023; 10:431
23. Ding Z, Li Y, Tang Z, et al. Role of gambogenic acid in regulating PI3K/Akt/NF- κ B signaling pathways in rat model of acute hepatotoxicity. *Biosci Biotechnol Biochem* 2021; 85:520-7.
24. Chen J, Li L, Zhou Y, et al. Gambogic acid ameliorates high glucose- and palmitic acid-induced inflammatory response in ARPE-19 cells via activating Nrf2 signaling pathway: ex vivo. *Cell stress chaperones* 2021; 26:367-75.
25. Khunpatee N, Bhukhai K, Chatsudhipong V, et al. Potential Application of Gambogic Acid for Retarding Renal Cyst Progression in Polycystic Kidney Disease. *Molecules (Basel, Switzerland)* 2022; 27.
26. Tang L, Li K, Zhang Y, et al. Quercetin liposomes ameliorate streptozotocin-induced diabetic nephropathy in diabetic rats. *Sci rep* 2020; 10:2440.
27. Tu Q, Li Y, Jin J, et al. Curcumin alleviates diabetic nephropathy via inhibiting podocyte mesenchymal transdifferentiation and inducing autophagy in rats and MPC5 cells. *Pharm Biol* 2019; 57:778-86.
28. Thongrung R, Pannangpetch P, Senggunprai L, et al. Moringa oleifera leaf extract ameliorates early stages of diabetic nephropathy in streptozotocin-induced diabetic rats. *J Appl Pharm Sci* 2023;13:158-66.
29. Liu Q, Shan P, Li H. Gambogic acid prevents angiotensin II-induced abdominal aortic aneurysm through inflammatory and oxidative stress dependent targeting the PI3K/Akt/mTOR and NF- κ B signaling pathways. *Mol Med Rep* 2019; 19:1396-402.
30. Mou Z, Feng Z, Xu Z, et al. Schisandrin B alleviates diabetic nephropathy through suppressing excessive inflammation and oxidative stress. *Biochem Biophys Res Commun* 2019; 508:243-9.
31. Ren J, Li L, Wang Y, et al. Gambogic acid induces heme oxygenase-1 through Nrf2 signaling pathway and inhibits NF- κ B and MAPK activation to reduce inflammation in LPS-activated RAW264.7 cells. *Biomed Pharmacother* 2019; 109:555-62.

32. Zhang H, Yang Y, Wang Y, et al. Renal-protective effect of thalidomide in streptozotocin-induced diabetic rats through anti-inflammatory pathway. *Drug Des Devel Ther* 2018; 12:89-98.
33. Qi Q, You Q, Gu H, et al. Studies on the toxicity of gambogic acid in rats. *J Ethnopharmacol* 2008; 117:433-8.
34. Guo Q, Qi Q, You Q, et al. Toxicological studies of gambogic acid and its potential targets in experimental animals. *Basic Clin Pharmacol Toxicol* 2006; 99:178-84.
35. Chi Y, Zhan XK, Yu H, et al. An open-labeled, randomized, multicenter phase IIa study of gambogic acid injection for advanced malignant tumors. *Chin Med J* 2013; 126:1642-6.
36. Liu W, Du JJ, Li ZH, et al. Liver injury associated with acute pancreatitis: The current status of clinical evaluation and involved mechanisms. *World J Clin Cases* 2021; 9:10418-29.
37. Wang H, Zhao Z, Lei S, et al. Gambogic acid induces autophagy and combines synergistically with chloroquine to suppress pancreatic cancer by increasing the accumulation of reactive oxygen species. *Cancer Cell Int* 2019; 19:7.